

A differential scanning calorimetry study of recrystallization and its interaction with precipitation in Al-Fe-Si commercial alloys (AA1145 and AA8011)

C. GARCÍA-CORDOVILLA, E. LOUIS

Centro de Investigación y Desarrollo, c/o Empresa Nacional del Aluminio, SA, Apartado 25, 03080 Alicante, Spain

Differential scanning calorimetry (DSC) was used to study several aspects of recrystallization in cold-rolled Al-Fe-Si commercial alloys. Two commercial alloys (AA1145 and AA8011) with different contents of Fe + Si and continuously cast in a twin roll machine, were used. It is shown that DSC allows a direct study of the interaction between the precipitation of alloying elements and recrystallization. The kinetics of recrystallization in the two alloys was also analysed, showing that the experimental data can be satisfactorily fitted with the Johnson-Mehl-Avrami equation with an exponent $n = 2.5$. The same kinetic parameters can be also used to fit the isothermal data obtained in the same DSC apparatus. The change in stored energy as a function of true strain is also considered.

1. Introduction

The measurement of the energy stored in plastically deformed metals has been, for the last twenty-odd years, a useful tool for the study of both the mechanism of plastic deformation and the processes of recovery and recrystallization [1-3]. The energy stored during deformation is that used in the formation of lattice defects (dislocations and vacancies), and therefore it remains in the metal [1]. All the methods used to measure the stored energy have been criticized and no one method is universally accepted [1-3]. One common method consists in putting the sample into the calorimeter after deformation [3]. This is the so called two-step method; the measurements can be made either isothermally or during a linear heating. In the latter case, recovery and recrystallization kinetics can be analysed at the same time. It should be noted that, since a great percentage of the stored energy is released during the recrystallization process (about 90%, see [1, 2]), the linear heating method is not the most suitable for the study of recovery, as it is impossible to study it separately from recrystallization. The most adequate method for the study of recovery would be the isothermal method at low temperature [1, 2].

The study of the stored energy in aluminium alloys [1-6] has not received as much attention as other metallurgical questions [4]. In particular, whereas modern differential scanning calorimetry (DSC) techniques are being widely used for the study of the precipitation and redissolution of phases in alloys [4, 7, 8] it has rarely been applied to the measurement of stored energy [6]. The purpose of this work is to carry out a study of recrystallization in Al-Fe-Si commercial alloys by means of the measurement of

stored energy [9-11] using DSC. An interesting aspect of commercial alloys, as compared to pure metals or diluted alloys, is the fact that depending on the state of the alloying elements (in solution or forming particles) they would interact in one way or another with recrystallization. This characteristic presents problems as the release (absorption) of energy during precipitation (redissolution) of phases can overlap and be much more important than in recrystallization processes.

The study was carried out on two continuously cast alloys with different percentages of Fe + Si (AA1145 and AA8011). In a recent investigation, the present authors [9] showed that the two exothermal reactions which appeared in the DSC curves for cold-worked alloys of the 1000 series, cannot be solely ascribed to recovery and recrystallization, respectively, as suggested by Hildebrandt [6]. In particular, although the second and strongest exothermal reaction is, in fact, related to recrystallization, the first would be mainly associated with precipitation of iron and/or silicon. One of the aims of this work with a higher Fe + Si alloy (AA8011) is to provide further support for the aforementioned interpretation since the reactions associated with precipitation and redissolution of phases will be markedly increased. Besides the interaction of precipitation and recrystallization, other aspects of the subject such as recrystallization kinetics and the stored energy as a function of true strain will also be investigated.

2. Materials and experimental procedures

The two alloys used in this work had been continuously cast in a twin-roll caster into a 1200 mm ×

8 mm slab at a speed of 1.2 m min^{-1} . Atomic absorption gave the following compositions (wt %): 0.31 Fe, 0.11 Si, 0.01 Mg, 0.05 Mn, 0.02 Zn, 0.015 Ti and 0.015 Cu for the AA1145 alloy, and, 0.66 Fe, 0.59 Si, 0.007 Mg, 0.03 Mn, 0.016 Zn, 0.017 Ti and 0.012 Cu for the AA8011 alloy. Some material was 85% cold rolled in a laboratory rolling mill, whereas other samples were annealed for 2 h after 60% cold reduction, and then 85% cold rolled. Annealing temperatures were in the range 200 to 600°C . In order to study the variation of stored energy as a function of true strain, measurements on samples subjected to intermediate annealing and 60 to 90% cold rolled were also made. Heat treatments were carried out in an air furnace, the temperature being controlled within $\pm 5^\circ\text{C}$.

The DSC measurements were performed using a Perkin-Elmer DSC-2C apparatus controlled through a minicomputer. Runs were carried out at heating rates in the range 5 to $80^\circ\text{C min}^{-1}$ and under dynamic argon atmosphere (1 litre h^{-1}). High purity aluminium was used as reference. Samples for DSC measurements were discs, 5 mm diameter, punched from the rolled sheet. It was checked that the deformation involved in the punching operation, although liable to affect the precipitation of phases in heat-treatable alloys [10, 11], does not affect either the measurement of stored energy or the precipitation of iron and/or silicon found in the course of this investigation (see next section). In some cases (especially for AA1145 alloy) and in order to increase the sensitivity, the base line was adjusted in the narrowest range possible and no crucibles were used for DSC runs up to 450°C ; above this temperature, the samples were placed in graphite crucibles. Isothermal experiments were carried out in the same DSC apparatus. There are two main difficulties with isothermal runs, (i) the loss of stored energy during the heating up to the desired temperature, and (ii) the time needed for sample equilibration. To reduce the effects of these two difficulties to a minimum, a medium heating rate ($80^\circ\text{C min}^{-1}$) was used up to 100°C below the chosen temperature and then a higher one ($320^\circ\text{C min}^{-1}$).

To check whether precipitation occurred during annealing, the electrical conductivity was measured by means of a Sigmatest-T instrument type 2067, and samples prepared as described by Howe [12], were examined by means of a Philips 500 Scanning Electron Microscope (SEM). In order to study the microstructural changes along a DSC run, samples were taken out from the DSC apparatus and quenched in water at room temperature. The microstructure of the samples was then studied by means of optical microscopy, SEM and Vickers micro-hardness measured on the sample surface, a load of 10 g was used (approximate size of the indentations $20 \mu\text{m} \times 20 \mu\text{m}$).

3. Results and discussion

3.1. Interpretation of DSC curves: interaction between precipitation and recrystallization

The DSC curves for samples without intermediate anneal show for both alloys a similar structure, namely, two distinct exothermal reactions followed by

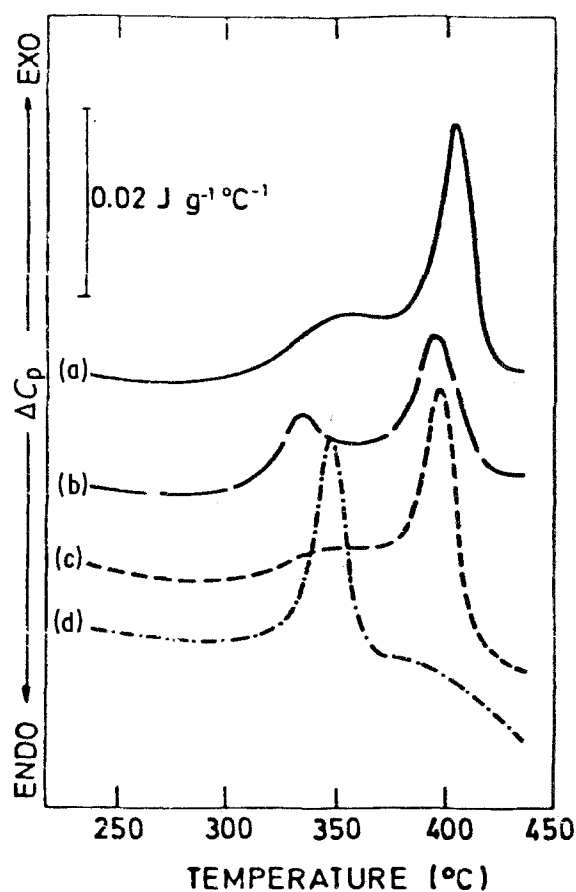


Figure 1 DSC curves for AA1145 alloy 85% cold rolled: (a) samples without intermediate anneal, (b, c, d) samples with 2 h intermediate anneal at 200, 400 and 600°C respectively, after 60% reduction. Heating rate: $40^\circ\text{C min}^{-1}$.

an endothermal one (Figs. 1 to 4 and Table I). It should be noted that the first and the last reactions are much stronger in the alloy with higher Fe + Si content (AA8011). In order to increase sensitivity, the DSC curve for AA1145 alloy was studied at temperatures below 450°C , therefore the third reaction is not visible in Fig. 1. The effect of the intermediate anneal at 400°C is very interesting: (i) it reduces, almost eliminates, the first exothermal reaction, and (ii) the second reaction is shifted around 60°C down to lower temperatures. Other annealing temperatures do not suppress the first peak, they only change its shape and diminish it, and they do not affect the second exothermal peak. On comparing the results for both alloys, it is worthwhile to note that the second exothermal peak occurs at lower temperatures for alloy AA8011 (Table I).

TABLE I Peak temperature ($^\circ\text{C}$) for the second exothermal reaction in Figs 1 and 2. Length of anneal: 2 h. Heating rate of the DSC run: $40^\circ\text{C min}^{-1}$

Intermediate annealing ($^\circ\text{C}$)	AA1145	AA8011
—	403	380
200	393	371
300	—	367
400	346	307
500	369	335
600	395	373

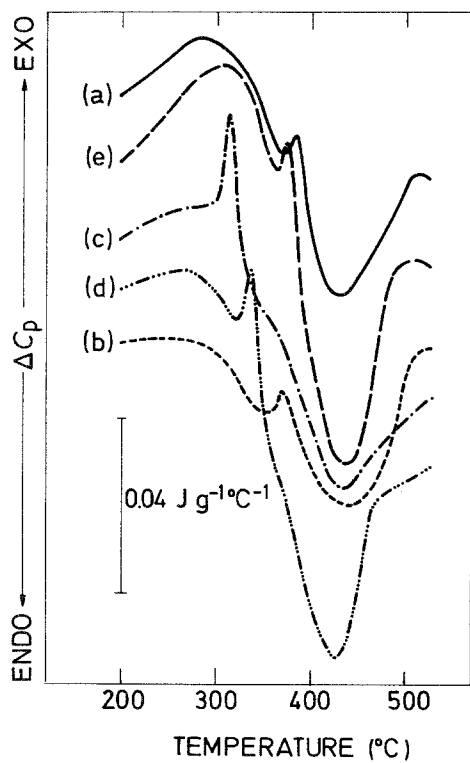


Figure 2 As Fig. 1 for AA8011 alloy. (b, c, d, e) correspond in this case to intermediate annealing at 300, 400, 500 and 600°C. Heating rate: 40°C min⁻¹.

The interpretation of the DSC curves was aided by carrying out further experiments in order to identify microstructural changes promoted by intermediate annealing and occurring during the DSC run. The study of the microstructure by means of SEM shows that the unannealed samples had a rather uniform distribution of very small particles (< 0.5 μm) and few particles > 1 μm. Annealing at 300 to 400°C strongly increases the number of large particles (> 1 μm) and reduces, to nearly zero, the number of small particles. Samples annealed at 600°C had a number of large particles with sizes between those for unannealed and 400°C annealed samples, and practically no small particles. These changes are naturally more substantial in AA8011 alloy. The above mentioned results are

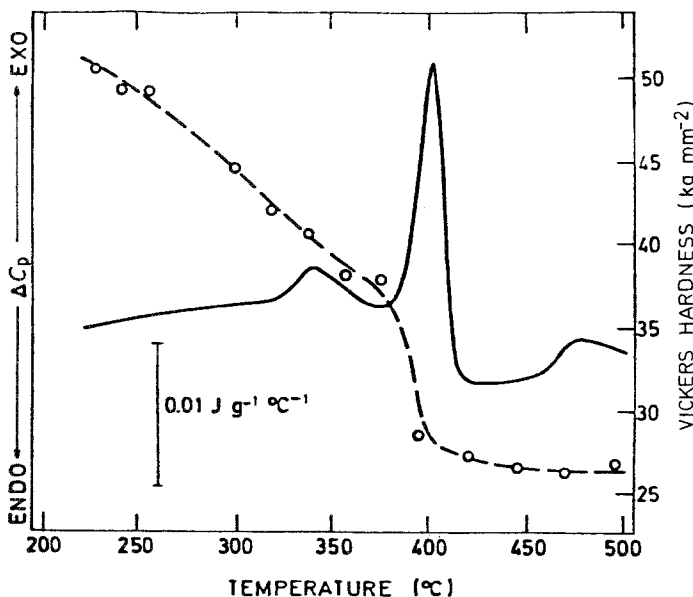


Figure 3 DSC curve for AA1145 alloy 85% cold rolled without intermediate annealing. Heating rate: 40°C min⁻¹. Measurements of Vickers hardness during the DSC run carried out at room temperature on samples taken out of the DSC apparatus and quenched.

in good agreement with measurements of electrical conductivity given in Fig. 5, the maximum precipitation given in Fig. 5, the maximum precipitation occurred around 300°C for AA8011 and above 350°C for AA1145.

Samples heated up to a given temperature in the DSC apparatus and quenched in water at room temperature, were first examined by means of optical microscopy. Recrystallization was observed to occur at temperatures coinciding with the main exothermic peak (Figs. 1 and 2), some recovery of the deformed structure was noticed at lower temperatures. These observations are in accordance with the Vickers hardness (VH) data shown in Fig. 3; a strong drop in VH is noticed coinciding with the main exothermic peak. The steady and less pronounced decrease in VH for lower temperatures might be related to both recovery and precipitation, although this correlation is not straightforward. It was possible to detect by means of SEM an overall increase in the number of particles in the range of the first exothermic peak and a decrease coinciding with the endothermic one.

These observations provide an interpretation of the three peaks. The third peak (endothermic) should account for the redissolution of phases. The main exothermic peak (second) is related to recrystallization whereas the first exothermic peak might be, in principle, associated with both recovery and precipitation processes. Nevertheless, the absence of the first peak in the DSC curves for AA1145 samples annealed at 400°C and the maximum conductivity (σ) reached at this temperature (Fig. 5) clearly suggests that this peak is mainly related to precipitation processes (note that the percentage of energy released during recovery is very small and difficult to detect as may occur in a very large temperature range). The AA8011 samples annealed at 400°C behave otherwise, as in this case the first peak, although very weak, still appears. This result must be interpreted taking into consideration the variation of σ with the annealing temperature for alloy AA8011 (Fig. 5). In this alloy the maximum σ is reached at 300°C, instead of 400°C, this indicates that maximum precipitation occurs at the lower temperature. On the other hand, considering that for

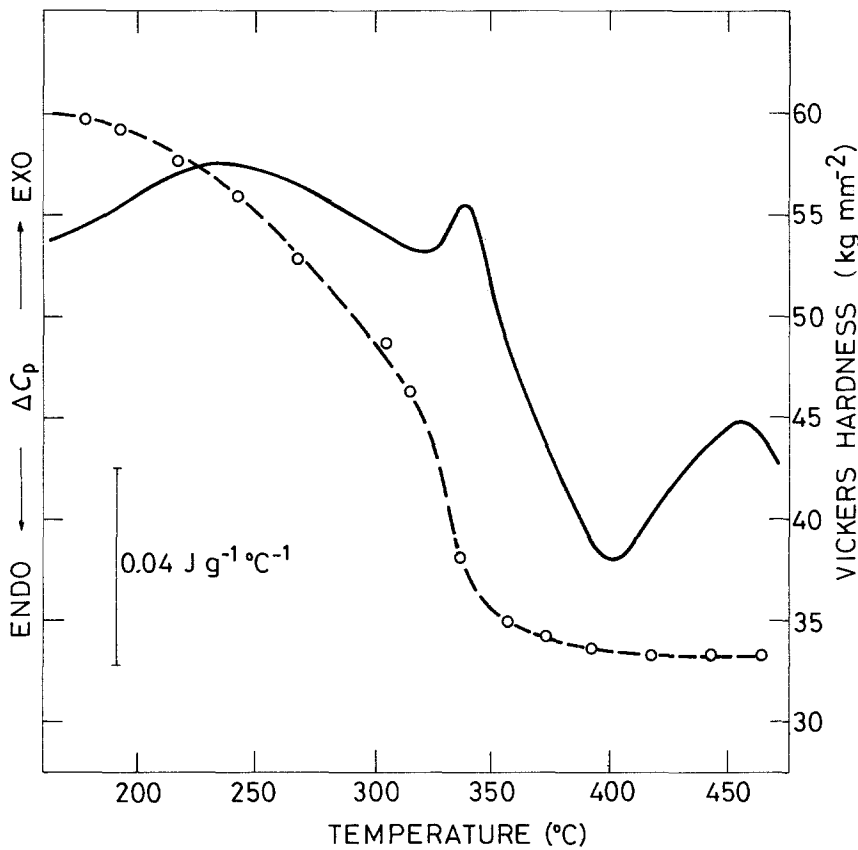


Figure 4 As Fig. 3 for AA8011 alloy 85% cold rolled without intermediate annealing. Heating rate: $5^{\circ}\text{C min}^{-1}$.

samples annealed at 300°C for 2 h, (i) the first exothermal peak still remains, and (ii) the second peak appears at higher temperatures than in samples annealed at 400°C , it can be concluded that 2 h is not long enough to precipitate all the elements in solution. Therefore the time at 300°C was varied, obtaining the results reported in Fig. 6 and Table II. Above 8 h of annealing a single peak remains, as obtained for 400°C , supporting the aforementioned interpretation of the first exothermic peak in terms of precipitation processes. Reasons why recrystallization for samples subjected to intermediate annealing at 400°C occurs at such low temperatures despite the fact that the first peak is still present, are discussed at the end of this section.

Results shown in Fig. 7 provide a further support for the interpretation of the first exothermal peak in terms of precipitation processes. This figure shows DSC curves for a cold-rolled sample of AA8011 alloy without intermediate anneal, and an as-cast sample. The latter DSC curve shows only two reactions accounting for precipitation (exothermal) and redissolution (endothermal) of phases; the precipitation reaction is weaker and occurs at temperatures higher than in the case of the cold-rolled sample (Fig. 7). This is readily understood by considering that plastic deformation favours the precipitation of phases [1].

The above interpretation of DSC curves allows us to understand the following points, (1) the first and third peaks are much more noticeable in the AA8011

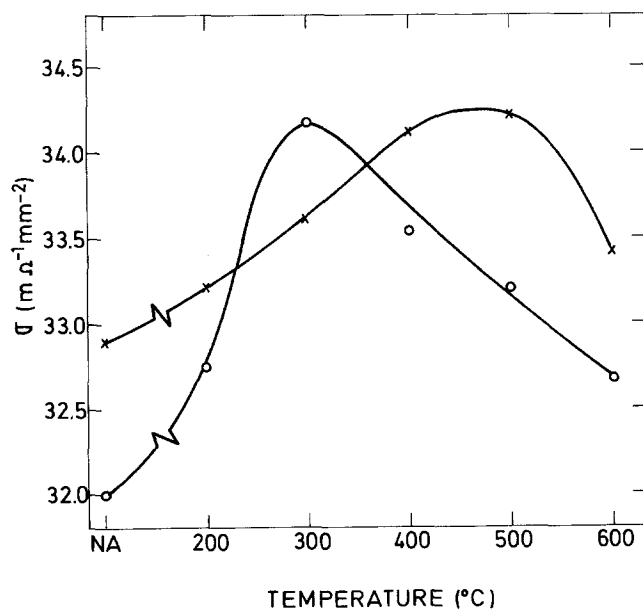


Figure 5 Change in electrical conductivity for (x) AA1145 and (o) AA8011 alloys (60% cold worked) as a function of isochronal anneals (2 h) at different temperatures.

TABLE II Peak temperatures of the main exothermal reaction for alloy AA8011 85% cold rolled after intermediate annealing at 300°C. The number of exothermal reactions is also indicated. Heating rate of the DSC run: 40°C min⁻¹

Annealing time (h)	Peak temperatures (°C)	Exothermal peaks
0.5	371	2
1	367	2
2	365	2
5	328	2
8	320	1
24	314	1

alloy as its Fe + Si content is higher (see Section 2); (2) when maximum precipitation occurs the first exothermic peak disappears (Figs. 3 and 6); and, (3) the shifting of the second peak (recrystallization) to lower temperatures is related to the disappearance of the first peak; this correlation can be understood by recalling that precipitation retards recrystallization [1–3]. However, for alloy AA8011 annealed at 400°C, recrystallization occurs at lower temperatures than in samples annealed at 300°C for 2 h, although the former have a higher supersaturation as the conductivity results indicate (Fig. 5). This result must be a consequence of another factor: particle size. It is well established that large particles (actual size depends on alloy) speed up recrystallization [1]. Then, as particles are larger for samples annealed at 400°C, they recrystallize at lower temperatures. A quantitative study of this point would require a careful analysis of the microstructure beyond the scope of the present work. Finally it is worth remarking that the recrystallization of AA8011 at lower temperatures (Table I) is a consequence of the higher density of particles acting as recrystallization nuclei; this factor overcomes the retarding effect of the higher supersaturation in AA8011 alloy.

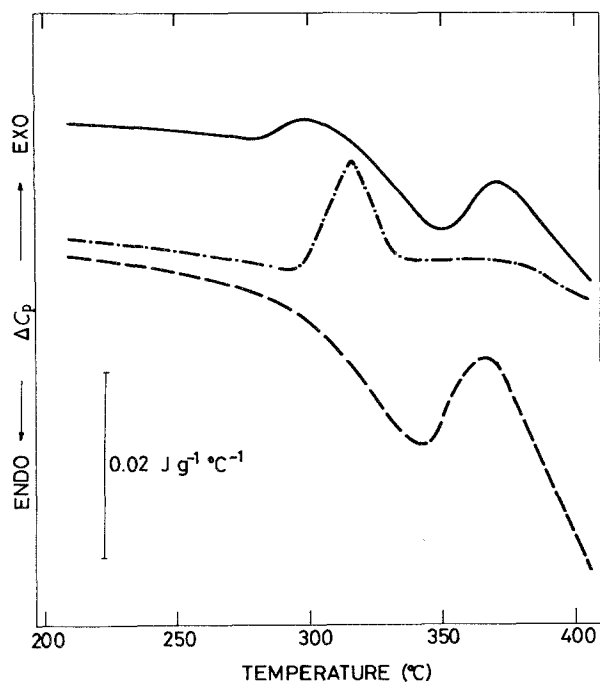


Figure 6 DSC curves for AA8011 alloy (85% cold rolled) subjected to an intermediate anneal at 300°C, at soak times of (—) 0.5 h, (---) 2 h, (- - -) 24 h. Heating rate: 40°C min⁻¹.

TABLE III Peak temperatures (°C) of the recrystallization reaction (main exothermal reaction) for samples of AA1145 and AA8011 with and without intermediate anneal at 400°C for 2 h, as a function of the heating rate of the DSC run. 85% deformation after intermediate annealing

	Intermediate anneal (°C)	Heating rate (°C min ⁻¹)					
		5	10	20	40	60	80
AA1145	—	367	378	391	406	413	418
	400	319	328	339	349	354	359
AA8011	—	345	356	368	380	386	388
	400	286	292	299	307	310	314

Before ending this subsection, it is worthwhile to point out that the interaction between precipitation and recrystallization in Al–Fe–Si alloys has been previously discussed by other authors (see [1], pp. 183 and 254). The merit of the present study relies upon the use of modern DSC techniques, and the demonstration that this technique is, in fact, a powerful tool for the study of recrystallization in both two-phase and supersaturated alloys [1].

3.2. Kinetics of recrystallization

The quantitative analysis of the second exothermal peak allows a study of the kinetics of recrystallization. Although, in principle, two different kinetics should be considered, namely nucleation and growth [1], the utilization of an “effective” kinetic is much simpler and has been also undertaken by several authors [1, 2]. The latter approach has been adopted in this paper.

The reaction rate is described by means of the Johnson–Mehl–Avrami equation [1, 2, 13],

$$\frac{d\alpha}{dt} = n(1 - \alpha)[- \ln(1 - \alpha)]^{(n-1)/n} \times [\nu \exp(-\Delta E/RT)] \quad (1)$$

where α is the fraction recrystallized, ν the frequency factor, ΔE the activation energy and n an exponent associated with the rate of nucleation and grain growth. Finally, R is the gas constant and T the absolute temperature.

The kinetic parameters ν , ΔE and n were determined in two steps. First, ν and ΔE were determined, following Kissinger’s method [2]. This method assumes that the reaction rate is maximum at the peak of the DSC curve (which holds true for DSC, see [14]). This assumption leads to the following equation [13]:

$$\ln \frac{h}{T_p^2} = -\frac{\Delta E}{RT_p} + \ln \frac{\nu R}{\Delta E} \quad (2)$$

where h is the heating rate and T_p the peak temperature. In this manner, varying h , ΔE and ν can be obtained by means of linear regression. Table III gives the peak temperatures (T_p) for different heating rates, and Table IV reports the results obtained for ΔE and

TABLE IV Activation energy ΔE and frequency factor ν calculated from the data of Table III, by means of the peak temperature method (see text), for samples with and without intermediate annealing (IA)

	IA (°C)	ΔE (kJ mol ⁻¹)	ν (min ⁻¹)
AA1145	—	183.4	2.7×10^{14}
	400	204.1	3.7×10^{17}
AA8011	—	198.8	2.0×10^{16}
	400	259.5	9.6×10^{23}

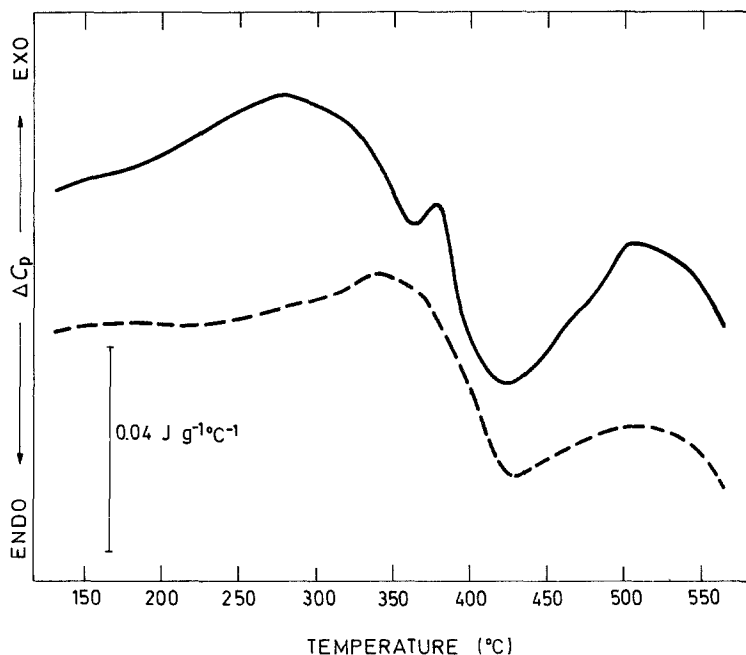


Figure 7 DSC curves for samples of alloy AA8011 either (---) as-cast or (—) after 85% cold rolling. Heating rate: 40° C min⁻¹.

ν by means of Equation 2. For both alloys, unannealed samples and samples subjected to an intermediate annealing at 400° C for 2 h were used. The peak-temperature method [13] allows the determination of ΔE and ν even in cases where two different reactions overlap (unannealed samples). Instead, n has to be adjusted to fit the fraction reacted given by the DSC curve. As this adjustment is rather unreliable for unannealed samples, we shall assume that the exponent n obtained for annealed samples is also valid for unannealed samples. This assumption allows a full description of kinetics for the two cases.

As mentioned above, the experimental results for the fraction reacted $\alpha(T)$ are adjusted to obtain the exponent n . $\alpha(T)$ is obtained from the DSC curve ($\Delta C_p(T)$), as follows:

$$\alpha(T) = \frac{\int_{T_0}^T dt \Delta C_p(T)}{A} \quad (3)$$

where A is the total peak area and T_0 the starting temperature.

The analytical expression for $\alpha(T)$ can be obtained by integrating Equation 1, considering that under non-isothermal conditions $T = T_0 + ht$, T_0 being the initial temperature [13],

$$\alpha(T) = 1 - \exp \left\{ - \left[\frac{\nu \Delta E}{Rh} P(x) \right]^n \right\} \quad (4)$$

where

$$x = \frac{\Delta E}{RT}, \quad P(x) = \int_x^\infty dx \frac{e^{-x}}{x^2} \quad (5)$$

In the adjustment of $\alpha(T)$, the experimental ΔE and ν values given in Table IV were used. The adjustment process is shown in Figs. 8 and 9 for AA1145 and AA8011 alloys, respectively. The n value is 2.5 for both alloys. This value adjusts satisfactorily $\alpha(T)$ for different heating rates. It is worthwhile to note that this n value is in good agreement with Avrami's analysis [1], which indicates that n should be between 2 and 3 for two dimensions and 3 to 4 for three dimension [1]. The dimension must be understood in terms of

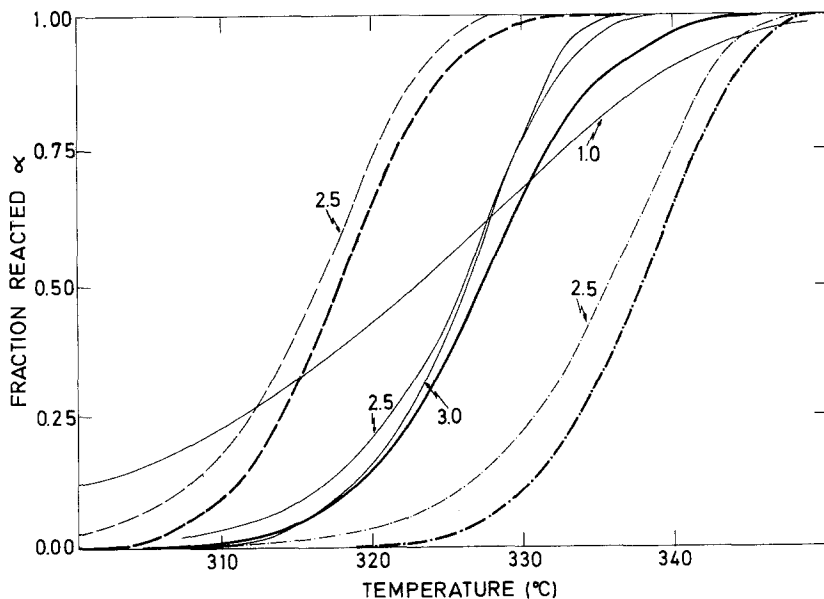


Figure 8 Fraction recrystallized for AA1145 alloy with intermediate anneal at 400° C (Fig. 1c). Adjustment of exponent n (see text). Heating rates of (---) 5° C min⁻¹, (—) 10° C min⁻¹, (-·-) 20° C min⁻¹.

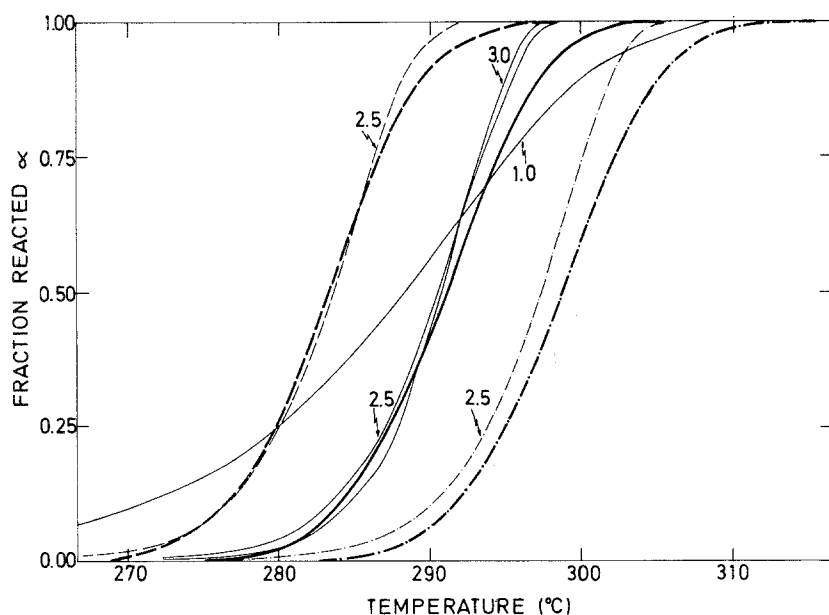


Figure 9 Fraction recrystallized for AA8011 alloy with intermediate anneal at 400° C (Fig. 2c). Adjustment of exponent n (see text). Heating rates of (---) 5° C min⁻¹, (—) 10° C min⁻¹, (- - -) 20° C min⁻¹.

grain size. Considering that the grain size in the alloys studied in this paper, ranges between 100 and 150 μm and the thickness of the sample studied was 500 μm , it is clear that in the present case, the samples are closer to two than to three dimensions.

3.3. Comparison between isothermal and non-isothermal kinetics

In order to check the validity of the kinetic parameters obtained, isothermal DSC measurements were also made. The difficulties encountered in isothermal measurements, essentially a consequence of the heating to the required temperature, were overcome following the procedure outlined in Section 2.

Only AA1145 alloy subjected to an intermediate annealing at 400° C for 2 h was studied, selecting temperatures of 307 and 317° C. Both recovery and recrystallization occur at those temperatures. Nevertheless, a result closely related to recrystallization can be obtained (Section 3.2) as follows. On the one hand,

the percentage of released energy associated to recovery is very small (10% of total stored energy). On the other hand, the kinetics of both processes are very different, then, supposing that both kinetics can be described following Avrami's equation [1], for recovery $n = 1$, whereas for recrystallization it would be > 1 [1]. These facts suggest that, while the reaction rate $d\alpha/dt$ (proportional to ΔC_p) for recovery should decrease monotonically, it should have a maximum for recrystallization. The value of this maximum was considered reliable and related to recrystallization.

Fig. 10 gives experimental data obtained by means of DSC. Fig. 11 shows the theoretical curves calculated using the kinetic parameters obtained in the non-isothermal experiments, as well as values for the maximum (experimental and theoretical). The agreement is highly satisfactory, substantiating the reliability of the analysis presented in this work.

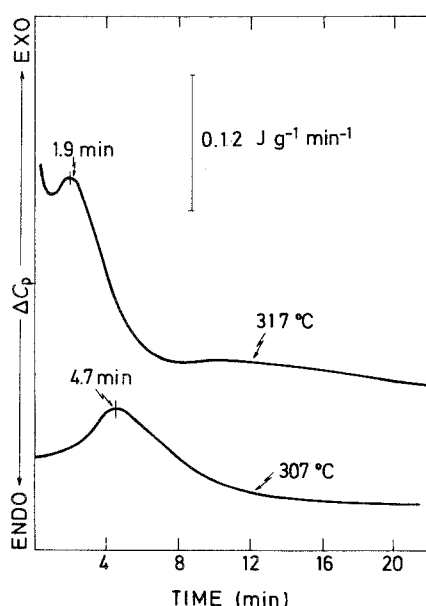


Figure 10 Reaction rate for AA1145 with intermediate anneal at 400° C, obtained through isothermal experiments carried out in the DSC apparatus.

3.4. Stored energy as a function of true strain

The measurement of the total energy stored during the deformation process is carried out only for samples subjected to the intermediate annealings leading to maximum precipitation (see Section 3.1). The following features of these results (Table V and Fig. 12) should be noted: (i) the stored energy varies more rapidly with true strain (ϵ) for alloy AA8011, due to the higher concentration of alloying elements which is known to increase the work hardening exponent, and (ii) the values for the stored energy are lower than those obtained by other authors for pure aluminium deformed under tension or torsion [5]. The latter point could be a consequence of the rolling operation which involves both compressive and shear stresses. On the

TABLE V Stored energy as a function of true strain (ϵ) for Al-Fe-Si alloys subjected to intermediate annealing at 400° C for 2h.

Alloy	Stored energy (J mol ⁻¹) for $\epsilon =$							
	0.22	0.29	0.41	0.69	0.80	1.10	1.20	1.39
AA1145	2.26	1.67	4.51	3.39	5.64	6.77	6.19	9.57
AA8011	1.13	2.26	4.51	10.16	9.03	12.42	12.42	13.54

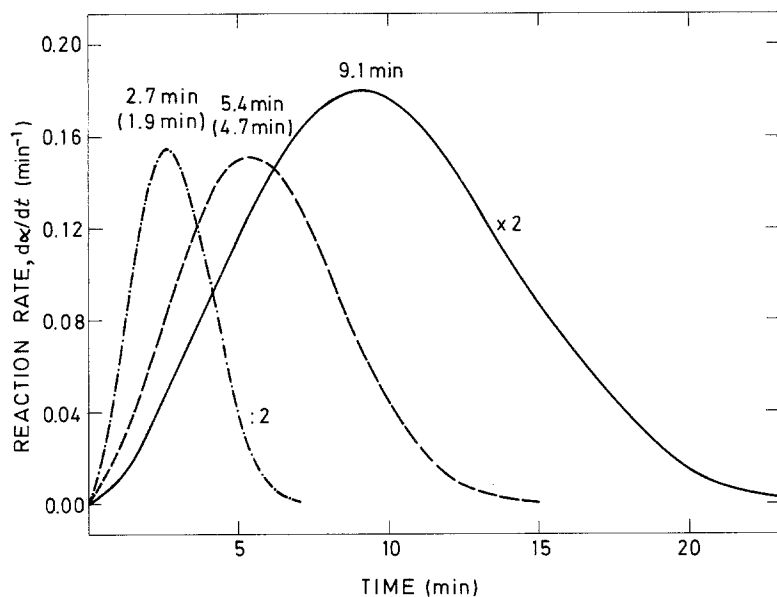


Figure 11 Isothermal reaction rate ($d\alpha/dt$) calculated by using the kinetic parameters obtained in non-isothermal experiments (Fig. 6). Values for time at which the reaction rate is maximum are shown in the figure, the experimental values shown in Fig. 10 are given in brackets. Alloy AA1145 subjected to an intermediate anneal at 400°C for 2 h. (---) $T = 317^\circ\text{C}$, (- - -) $T = 307^\circ\text{C}$, (—) $T = 300^\circ\text{C}$.

other hand, the way in which rolling is carried out affects dynamic recovery and hence the stored energy; in this work neither the passes nor the percentage reduction per pass were controlled. Finally it should be mentioned that the higher ϵ , the lower the recrystallization temperature; for instance the peak temperature for the alloy AA1145 subjected to true strains of 0.22 and 1.39 is 405 and 357°C , respectively; this is also in agreement with previous experience [1].

4. Conclusions

1. The DSC curves for cold-worked non-homogenized Al-Fe-Si (AA1145, AA8011) alloys, without intermediate anneals, show two exothermal and one endothermal reactions. The results of this work ascribe the first exothermal and the endothermal reactions to precipitation and redissolution of phases, respectively, whereas the second exothermal reaction corresponds to recrystallization. The weak energy released during the recovery can be overlapped with the first peak, therefore it is difficult to detect it.

2. The effects of an intermediate annealing are two: (i) it reduces the first exothermal reaction, (ii) it speeds

up the second exothermal reaction. Both effects can be easily understood by considering the interpretation of the DSC curves presented in the previous conclusion. The intermediate anneal favours precipitation, therefore eliminating the first peak. On the other hand, since the precipitation prior to recrystallization slows down the latter, the sample with intermediate anneal recrystallizes at lower temperatures than that not annealed.

3. The fraction reacted obtained from the DSC curves can be adjusted by means of the Johnson-Mehl-Avrami equation, with a value of 2.5 for the exponent n , in good agreement with Avrami's prediction. The kinetic parameters obtained in this manner lead also to a correct description of isothermal kinetics: the results are in full agreement with the experimental curves obtained with the same DSC equipment utilized in the isothermal mode.

4. Comparing the results obtained for the two alloys studied here, the following points should be noted: (a) AA8011 alloy recrystallizes at lower temperatures than AA1145, which must be a consequence of the higher density of particles that may act as recrystallization nuclei in the former; (b) the stored energy increases faster with true strain (ϵ) in the alloy with highest Fe + Si content (AA8011). This result is in agreement with the fact that this alloy has a higher work-hardening rate than AA1145 alloy.

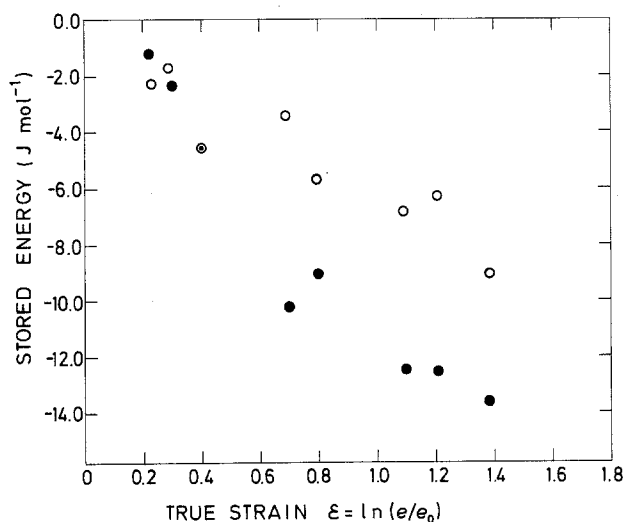


Figure 12 Stored energy as a function of true strain for (O) AA1145 and (●) AA8011 alloys, subjected to an intermediate annealing.

Acknowledgements

The authors are grateful to Alcan International Ltd for permission to publish this work. The assistance of R. Mora and J. Pastor in the electron and optical microscopy work is gratefully acknowledged.

References

1. P. COTTERILL and P. R. MOULD, "Recrystallization and Grain Growth in Metals" (Surrey University Press, London, 1976).
2. M. B. BEVER, D. L. HOLT and A. L. TITCHENER, *Prog. Mater. Sci.* **17** (1973).
3. L. M. CLAREBROUGH, M. E. HARGREAVES and M. H. LORETTO, in "Recovery and Recrystallization of Metals", edited by L. Himmel (Interscience, New York, London, 1963) p. 63.

4. L. F. MONDOLFO, "Aluminium Alloys: Structure and Properties", 1st Edn, (Butterworth, London, Boston, 1976).
5. C. M. ADAM and A. WOLFENDEN, *Acta Metall.* **26** (1978) 1307.
6. W. H. HILDERBRANDT, *Met. Trans.* **10A** (1979) 1045.
7. D. J. THOMPSON, "Thermal Analysis", Vol. 2, edited by R. T. Schwenker Jr and P. D. Garn (Academic, New York, London, 1969) p. 1147.
8. K. HIRANO, in "Thermal Analysis: Comparative studies on Materials", edited by H. Kambe and P. D. Garn (Wiley, New York, 1974) p. 42.
9. C. GARCÍA-CORDOVILLA and E. LOUIS, *Scripta Metall.* **18** (1984) 549.
10. *Idem*, *Met. Trans.* **15A** (1984) 389.
11. *Idem*, *Scripta Metall.* **18** (1984) 291.
12. J. HOWE, *Metallography* **16** (1983) 275.
13. D. W. HENDERSON, *J. Non-Cryst. Solids* **30** (1979) 301.
14. E. LOUIS and C. GARCÍA-CORDOVILLA, *J. Mater. Sci.* **19** (1984) 689.

*Received 4 March
and accepted 31 May 1985*